



Research Article

Analysis of solar water desalination using hybrid nanofluids: An experimental study

Ajit^{1,2}, Harshit PANDEY³, Naveen Kumar GUPTA^{1,*}

¹Department of Mechanical Engineering, GLA University, Mathura, 281406, India

²Department of Mechanical Engineering, Manav Rachna University, Faridabad, 121004, India

³Department of Mechanical Engineering, Bundelkhand Institute of Engineering & Technology, Jhansi, 284128, India

ARTICLE INFO

Article history

Received: 17 April 2022

Accepted: 28 May 2022

Keywords:

Water Purification; Hybrid Nanofluid; Solar Heater; Pyramid Solar Still; Fresh Water

ABSTRACT

The performance characteristics of a novel solar water desalination system has been investigated experimentally. The desalination unit consisted of a square basin-pyramid solar still coupled with a solar heater. Different DI water based mono and hybrid nanofluids were prepared using CuO and GO nanoparticles following the two-step method. DI water when employed as the heat transfer fluid in the system, improved the distillate water yield by about 28.80% relative to the conventional solar still. Out of all the considered CuO mono-nanofluids, the 1.0 wt.% concentration resulted in the maximum increment of about 78.80% in the distillate water yield followed by 1.5 wt.% (62.05%) and 0.5 wt.% (53.30%) respectively. Utilizing the CuO+GO hybrid nanofluid, resulted in maximum increment of about 127.46% at 25:75 nanoparticle proportion followed by, 50:50 (101.33%) and 75:25 (89.30%) respectively, while employing the 1.0 wt.% GO mono-nanofluid, resulted in an increment of about 54.93% in the distillate water yield. The pumping power of the prepared nanofluids was found to be the function of their concentration. Hence, the performance index was evaluated for all the tested heat transfer fluids followed by an economic analysis of all the considered cases. The purity of the produced distilled water was also assessed by comparing with the Bureau of Indian Standards. Finally, the study proposed the best suitable heat transfer fluid for the investigated system and suggested the possible futuristic research objectives.

Cite this article as: Ajit, Pandey H, Gupta NK. Analysis of solar water desalination using hybrid nanofluids: An experimental study. J Ther Eng 2023;9(6):1502–1515.

INTRODUCTION

The necessity of fresh water has been observed to prevail significantly in our society as one of the basic needs. The requirement of the same has observed a noticeable evolution to meet out the ongoing pace of industrialization

and growing human population. The World Health Organization reported that about 1.8 billion peoples would suffer from water scarcity by the year of 2025 [1]. The scarcity of consumable water has posed itself as a major point of concern among the environmentalists and the scientific

*Corresponding author.

*E-mail address: naveen.gupta@gla.ac.in

This paper was recommended for publication in revised form by Regional Editor Jaap Hoffman



researchers. The conventional systems and the primitive technologies employed for water desalination for the production of fresh water depend mainly on the usage of fossil fuels. The major issues associated with the fossil fuels are its ability to replenish and the adverse impact on the environment when utilized for different applications [2,3]. This necessitates the usage of non-conventional methods and sustainable energy resources in the water desalination. The solar-thermal energy is one of the widely discussed sustainable energy source among the researchers owing to its availability and performance potential.

Solar based water desalination systems act as potential cost-effective and effectively green solution for the production of fresh water without requiring any usage of fossil fuels [4]. The solar desalination systems can be employed in the regions which enjoy abundant incoming solar radiation. The solar distillers in their simplest construction consist of a base tank or basin filled with the impure water, a cover plate to collect the water vapor condensate. The solar stills utilize the incident solar radiation to carry out vaporization in the impure water filled in the distiller basin to produce water vapors. The produced water vapors move upwards and get collected over the distiller cover plate and get condensed resulting in production of fresh water. Several modifications have been carried out lately in the design structure of solar distillers like pyramid [5,6], inclined [7,8], double sloped [9,10] and stepped solar distillers [11,12] to attain high fresh water yield accompanied with enhanced thermal efficiency and low cost.

The usage of nanofluids and their influence on the performance characteristics in the solar based desalination applications has also been widely discussed lately. The nanoparticles have been reported in the literature to offer appreciable thermophysical characteristics accompanied with medicinal/chemical advantages in the water purification applications. Researchers have tried to utilize nanoparticles in the solar desalination-based water purification systems in the following ways:

- Purification of impure water using the anti-bacterial action of nanoparticles.
- Heat transfer augmentation across the impure water improving its thermophysical properties.
- Improving the solar radiation absorptivity of the system.
- Employing nano embedded phase change materials as energy storage materials.
- Nanoparticle coating on the absorber plate to improve the heat supply to the impure water.
- Cooling of the cover plates of the solar distillers.

Different nanoparticles like silver (Ag), copper (Cu), magnesium oxide (MgO), alumina (Al₂O₃), carbon nanotubes (CNT), silicon dioxide (SiO₂) etc. have been reported to be used by the researchers in different solar distillers. The performance of the solar distillers has also been tried to improve by carrying out certain modifications like employing thermoelectric heaters [13], energy storage materials

[14], heat pipes [15], wick [16], fins [17], collectors [18] etc. Nazari et al. [19] investigated the performance of a solar still using CuO nanofluid. The solar still glass cover was assisted with thermoelectric cooling. They reported that the modified solar still with added nanoparticles to the impure water offered improved fresh water yield relative that offered by the modified solar still without using the nanofluid. A maximum increment of about 81%, 80.6% and 112.5% was attained in the fresh water productivity, energy and the exergy efficiency respectively using the 0.08 vol. % copper oxide nanofluid in the modified solar still.

Shoeibi et al. [20] investigated the influence of nanofluid based thermoelectric heating-cooling on the productivity of solar stills. The thermoelectrically cooled nanofluids were employed to reduce the glass cover temperature while the thermoelectrically heated nanofluids were employed to increase the saline water temperature. It was found that the performance of the solar still advanced at higher nanofluid concentrations. A maximum increment of about 11.57% was attained in the fresh water productivity using the Al₂O₃ nanofluid in the modified solar still. Abdelgaied et al. [21] experimentally investigated the performance of a tubular solar still. They employed copper fins on the absorber surface and phase change material below the absorber surface and observed the performance of the solar still. It was found during the experimentation that employing the circular and the square shaped copper fins on the absorber plate improved the productivity of the solar still by about 47.2% and 33% respectively. They reported that employing the phase change material accompanied by circular fins resulted in the best desalination performance and improved the fresh water productivity by about 90.1%.

Abdelaziz et al. [22] studied the influence of employing corrugated aluminum basin, wick material, carbon black nanofluid, phase change materials and their combinations on a tubular solar still performance. They reported that the best solar still performance was attained employing the 1.5 wt.% carbon black nanofluid based wicked corrugated basin along with 3 wt.% carbon black nanoparticle embedded paraffin wax under the basin. They reported that modifying the solar still lead to a reduction of about 22.47% in the cost. Abdelgaied et al. [23] investigated the thermo-economic characteristics of a modified hemispherical solar still. The modifications were carried out by employing CuO nanofluid in the solar still basin, phase change material beneath the basin and their combination. They reported that using the CuO nanofluid and phase change material increased the productivity of the solar still by about 60.41% and 29.17% respectively. The best solar still performance with maximum productivity enhancement of about 80.20% was attained with the simultaneous use of CuO nanofluid and the phase change material in the solar still.

Shoeibi et al. [24] numerically studied the influence of glass cooling using Al₂O₃-TiO₂ hybrid nanofluid on the productivity of a double-slope solar still. Pumping the hybrid nanofluid over the glass cover increased the temperature

gradient between the glass cover and saline water, further improving the convective heat transfer within the solar still. An optimum nanofluid concentration of about 0.45% was found for the glass cooling after a CFD simulation. The fresh water yield, energy efficiency increased by about 11.09%, 28.21% respectively using the hybrid nanofluid for glass cooling. Rabbi et al. [25] studied the performance of a solar still assisted with a heat exchanger within the basin to carry out heat supply to the saline water. They prepared Al_2O_3 , CuO mono-nanofluids and $\text{Al}_2\text{O}_3\text{-CuO}$, $\text{Al}_2\text{O}_3\text{-SiO}_2$ hybrid nanofluids respectively and used them in the heat exchanger. They reported that the maximum fresh water productivity increment of about 298.3% was attained by employing the $\text{Al}_2\text{O}_3\text{-SiO}_2$ hybrid nanofluid within the heat exchanger in the solar still basin.

Thus, it becomes obvious post-discussion that the solar stills have a huge potential to offer appreciable performance by employing justified modifications in their arrangement. Nanofluids and especially the hybrid nanofluids can be used to augment the heat transfer to the saline water while offering enhanced thermophysical properties and improving the desalination process. However, the effect of direct mixing of the nanoparticles within the saline water to produce fresh water from may lead to certain health-related complications when consumed directly. To avoid such drawbacks, the nanofluids can be used as the thermo-fluids without directly interacting with the saline water to enhance the solar still performance while overcoming the health hazard related to the nanoparticle usage. Hence in the current study contemplates to enhance the performance of a pyramid solar still by coupling it with a solar heater and using mono, hybrid nanofluids as heat transfer fluids.

EXPERIMENTATION

Figures 1 and 2 represent the schematic and actual illustration of the experimental set-up respectively. The experimental set-up consisted of a square basin pyramid solar still and a solar heater connected with each other with a valves and pumping arrangement. The basin of the solar still was made to have an effective area of $0.6\text{m} \times 0.6\text{m}$ and depth 0.2m, fabricated using copper sheets. The absorber plate of the basin was painted black in color to augment the heat absorption. The basin of the tank was insulated using wood of thickness 0.025m. The glass cover plates of the solar still of 90% transmissibility were inclined at an angle of 25° with the horizontal level. The saline water level in the basin was maintained by regulating its supply via a valve further connected to a supply tank. The distilled water produced within the solar still was collected in a collection cum measuring jar through a valve by employing a collecting channel. Another valve was employed to drain out the brine water of the solar still. A hole was drilled in the solar still body to insert thermocouples for temperature measurement. All the thermocouples were further connected to a temperature indicator. The solar heater with a flat plate collector was fabricated using a glass cover plate (transmissibility=90%) inclined at 0° with the horizontal level. The basin of the solar heater was also fabricated using copper sheet and insulated using wood of thickness 0.025m. A network of black coated copper tube in serpentine arrangement was assembled within the heater, filled with heat transfer fluid. The flow of heat transfer fluid from the heater to the solar still was controlled using supply valve and maintained using a pump.

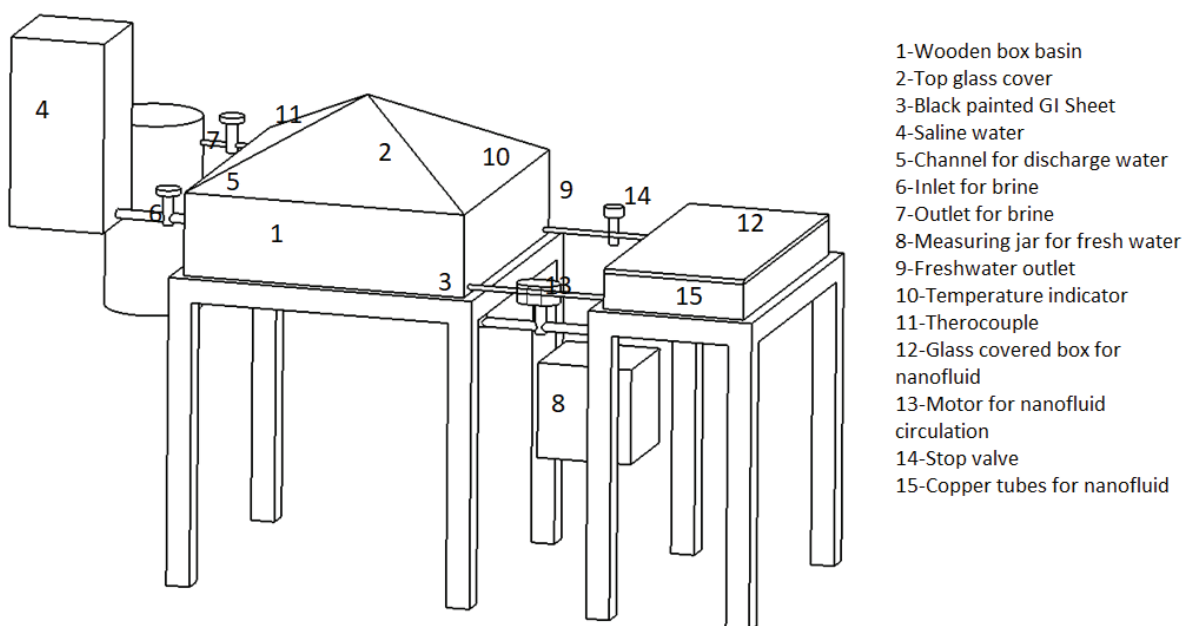


Figure 1. Schematic diagram of the experimental set-up.



Figure 2. Actual photograph of the experimental set-up.

Nanofluid Synthesis

All the mono-nanofluids (MNFs), hybrid nanofluids (HNFs) in the current work were prepared following the two-step method of nanofluid preparation. The prepared nanofluids were ultrasonicated for 2 hours each to confirm the proper dispersion of added nanoparticles in the base fluid (DI water). The MNFs and HNFs prepared in the present work and their respective concentrations, nanoparticle proportions are specified in Table 1.

Figure 3 (a-d) illustrate the SEM, TEM images of the utilized CuO and GO nanoparticles respectively. The CuO nanoparticles utilized were of average size of about 50nm while the GO nanoparticles were of average length 500nm and average thickness of about 5nm. All the prepared nanofluids were tested for stability through sedimentation visualization techniques. None of the prepared nanofluids showed distinct sedimentation up to 20 days, except the GO MNF that exhibited certain sedimentation at the 15th day from its preparation.

Experimental Procedure

The present work comprised of a series of experiments performed during the time period of 9:00 AM to 6:00 PM in the month of March, in the environmental conditions of Faridabad (28.4089° N, 77.3178° E), Haryana, India. The water level inside the basin effects the productivity of the solar still hence it was maintained at 0.05m during the whole experimentation. During the experimentation, the set-up was operated in two different modes. Initially the solar still was disengaged from the solar heater and operated while the further experiments were carried out on the solar heater coupled solar still. In the solar heater, different heat transfer fluids were filled and tested on by one in order to properly assess their effect on the solar still performance.

The experiment on the conventional solar still was carried out by filling the saline water in the basin and allowing the solar irradiation to cross the cover plate and heat the filled saline water. This eventually increased the temperature of the saline water favoring its evaporation. The

Table 1. Specifications of the nanofluids used in the present study

Nano-suspension	Nomenclature	Concentration	Nanoparticle Proportion
CuO MNF	MNF-1	0.5 wt.%	100% CuO
CuO MNF	MNF-2	1.0 wt.%	100% CuO
CuO MNF	MNF-3	1.5 wt.%	100% CuO
GO MNF	MNF-4	1.0 wt.%	100% GO
CuO+GO HNF	HNF-1	1.0 wt.%	75% (CuO) + 25% (GO)
CuO+GO HNF	HNF-2	1.0 wt.%	50% (CuO) + 50% (GO)
CuO+GO HNF	HNF-3	1.0 wt.%	25% (CuO) + 75% (GO)

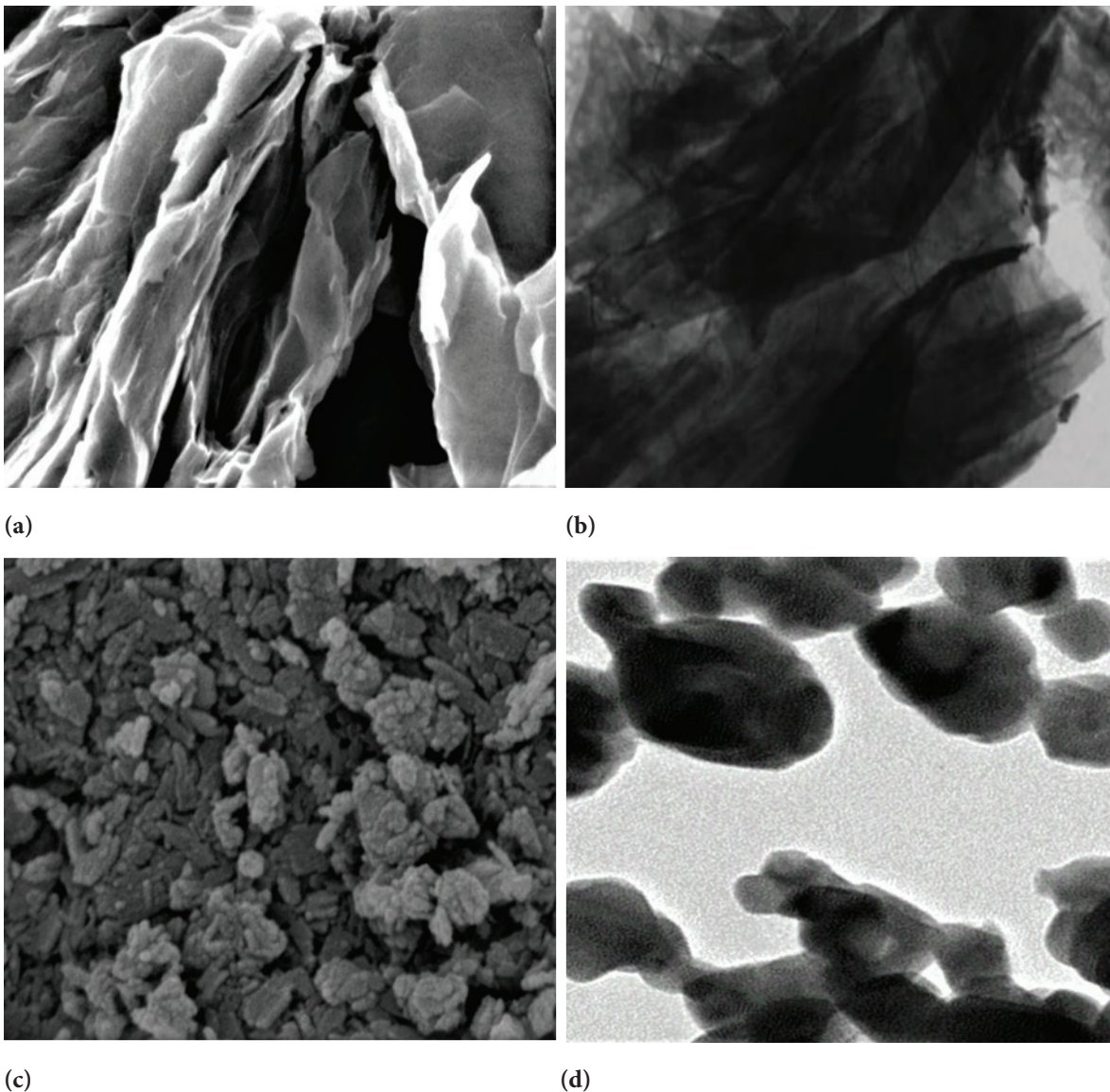


Figure 3. Microscopic images of nanoparticles (a) SEM image of CuO nanoparticles, (b) TEM image of CuO nanoparticles, (c) SEM image of GO nanoparticles (d) TEM image of GO nanoparticles.

produced water vapors then started to move upwards due to density difference towards the cover plate and got condensed over its inner surface due to temperature gradient between them. The distilled water in the form of condensate was then allowed to slide downwards through the inclined surface of the cover plate utilizing the gravitational force. Once the condensate reached at the bottom edge of the cover plate, it was collected and drained out of the solar still into a collection cum measuring jar through the collection arrangement.

The solar heater coupled solar still was also operated by following the procedure similar to that of the conventional solar still. However, in this operational mode the solar heater was also operated. In order to operate the solar heater, the tube of the solar heater was filled with heat transfer fluid

and then allowed to gain the thermal energy of the solar irradiation crossing the cover plate. Following it, the temperature of the heat transfer fluid increased significantly and then this high temperature heat transfer fluid was made to flow through the tube towards the solar still basin such that once the heat transfer fluid came in indirect contact of the saline water, the temperature of the latter increased appreciably by absorbing the heat energy rejected by the former. Such increment in the saline water temperature, augmented its rate of evaporation, further enhancing the fresh water productivity rate. The heat transfer fluid after releasing its sensible heat was then pumped back towards the solar heater through the closed network of the tube to maintain its cyclic flow.

Table 2. Technical details of the measurement devices.

Parameter	Device	Range	Accuracy	Uncertainty
Solar irradiation intensity	Solar power meter	0-2000 Wm ⁻²	± 5 Wm ⁻²	0.3
Wind speed	Anemometer	0-30 ms ⁻¹	± 0.1ms ⁻¹	0.1
Temperature	K-type thermocouples	0-600 °C	± 0.1 °C	0.05
Distillate water yield	Collection cum measuring jar	0-3000 cc	± 50 cc	0.15

The heat transfer fluids namely water, MNF-1, MNF-2, MNF-3, HNF-1, HNF-2, HNF-3, MNF-4 were filled one by one inside the tube of the solar heater and were investigated to identify the best out of all the investigated heat transfer fluids. In order, proper cleaning of the tube and pump was ensured. Proper cleaning of the whole experimental set-up was ensured to reduce the effect of a day of experiment over the another. It was necessitated to effectively avoid the influence of the usage of one heat transfer fluid over the other. The water temperatures, glass temperatures, distilled-water yields and the solar irradiation intensities were measured on hourly basis during the experiments. All the temperatures were measured employing the K-type thermocouples connected to a data-logger. The solar irradiation intensity was measured using a solar power meter. The technical specifications of all the measurement devices used during the experiment are specified in Table 2.

Uncertainty Analysis

The experiment method is an indirect way to estimate the performance of a solar still. This results in a significant uncertainty in the measurands. In order to properly assess the uncertainty in the measurands, the data of the distinct parameter was recorded was recorded during the experiment and an approximation for the uncertainty in the individual sample was calculated. The estimation of uncertainty (U_i) was carried out using the formula:

The principle of the photo-thermal energy conversion is converting the energy of the incident radiation to thermal energy, solar thermal systems collectors are one of the examples. The energy equation for the solar system collector, accounting for the volumetric heat release, can be written as:

$$U_i = \sqrt{\frac{\sum \sigma_i^2}{N^2}} \tag{1}$$

here, N is the total number of samples and σ_i is the standard deviation in ith sample. The system uncertainty is shown in Table 2. The obtained results may get effected by the thermal storage phenomena. The error caused due to thermal energy storage was calculated as:

$$Error (\%) = \frac{Distillate\ water\ yield\ in\ the\ absence\ of\ sunlight}{Distillate\ water\ yield\ in\ the\ presence\ of\ sunlight} * 100 \tag{2}$$

As the thermal energy storage effect was negligible since insignificant evaporation occurred in the absence of sunlight (during non-sunshine hours). Hence the error due to thermal energy storage came to be nearly equal to 0%.

RESULTS AND DISCUSSION

The solar irradiation intensities, wind speeds were recorded on hourly basis during the experiments to assess their respective variations. Figure 4 illustrates the variation in the incident solar radiation intensity and wind speed during the experiments where the error bars represent their fluctuation relative to their respective average values. It is clear from the figure that both the solar irradiation intensities, wind speeds were almost constant throughout the experimentation period, enabling effective comparison of different operational modes of the solar still in terms of the productivity. The incident solar radiation intensity and wind speed were found to climb up attain their peak values at 14:00 hours and 15:00 hours respectively.

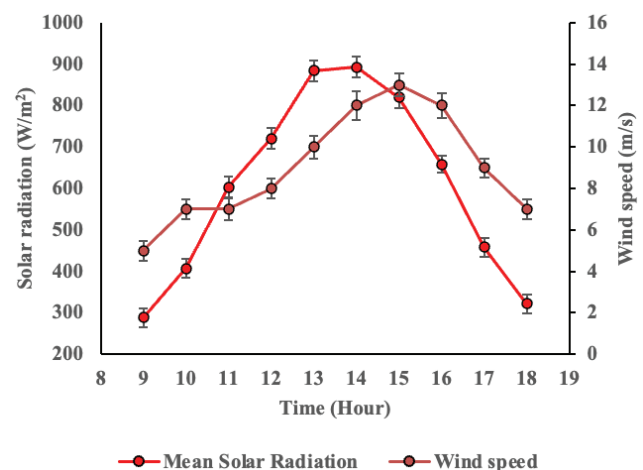


Figure 4. Average variation of solar irradiation intensity and wind speed with time during the experiment.

Figure 5 illustrates the hourly variation in the water, glass temperatures and production (distilled water yield) of conventional solar still (i.e., without engaging the solar heater) with solar irradiation intensity (Case 1). It is clear

from the figure that the production of distillate water in the solar still gets significantly influenced by the solar irradiation intensity. The trend of the distilled water yield varied exhibiting direct proportionality with that of the solar irradiation intensity at hourly basis. Similar to the trend of the distillate water yield, the water and the glass temperatures were also observed to increase with an increase in the solar irradiation intensity. The distillate water yield, water and glass temperature were recorded to showcase their respective peaks at 14:00 hours with the values of 236 cc, 58.2 °C and 44.9 °C respectively. In the initial hours of the experiment, the hourly difference between the water and glass temperatures were not much prevalent, attributed to the lower solar irradiation intensity during the same time period. However, with further progression in the time, the increment in the solar irradiation intensity was observed. This resulted in appreciable temperature difference between the the water and glass cover and eventually resulted in the improved distillate water yield.

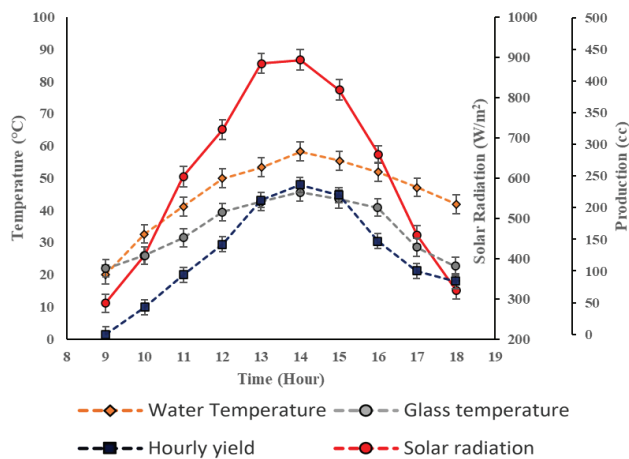


Figure 5. Variation of hourly yield and temperatures of conventional solar still with solar irradiation intensity.

The Figure 6 illustrates the hourly variation in the water, glass temperatures and distilled water yield (production) of solar heater coupled still with solar irradiation intensity using water as the heat transfer fluid (Case 2). The glass temperature variation in this arrangement was found to be almost similar to that in the Case 1, attributed to almost similar solar irradiation intensity. Similar to Case 1, the water temperature and distillate water yield of Case 2 were also observed to showcase direct proportionality with the solar irradiation intensity. This could be attributed to the dependence of the sensible heat absorbed by saline water and its evaporation rate on the intensity of the solar irradiation. Coupling the solar heater with the solar still increased the water temperature, attributed to the heat transfer from the high temperature water (of the solar heater) to the

saline water during the indirect contact with each other within the basin. It further augmented the evaporation rate of the saline water enhancing the productivity of the solar still. Using water as the heat transfer fluid (Case 2) resulted in a maximum increment of about 28.80% in the distillate water yield of solar still relative to that in Case 1.

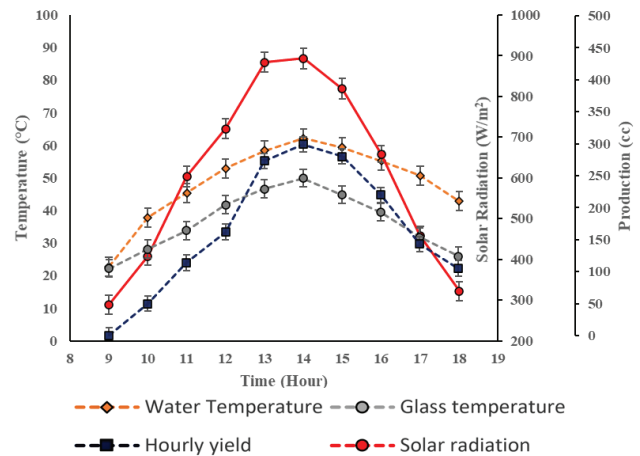


Figure 6. Variation of hourly yield and temperatures of solar still with solar intensity using water in the heater.

Figure 7 (a)-(c) illustrate the hourly variation in the water, glass temperatures and distilled water yield of solar heater coupled still with solar irradiation intensity using MNF-1 (Case 3), MNF-2 (Case 4) and MNF-3 (Case 5) respectively as the heat transfer fluids. The hourly distillate water yield in the Cases 3-5 were found to vary directly proportional with the solar irradiation intensity. The hourly distillate water yield was observed to be lower during the initial hours and attain peak at 14:00 hours in the Cases 3-5. It can be regarded to the lower solar irradiation intensity during the initial hours and attainment of peak value at 14:00 hours of a day. The water, glass temperatures were also observed to vary with the solar irradiation intensity and attained peak values at 14:00 hours. Using CuO MNFs as heat transfer fluids in the solar heater coupled still (Cases 3-5) significantly increased the saline water temperature relative to that attained in Cases 1, 2 respectively. This could be attributed to the additional supply of heat energy to the saline water due to utilization of CuO MNFs as heat transfer fluids. Another reason behind the improved performance of solar still in the Cases 3-5 could be attributed to superior thermophysical properties of the MNFs relative to that of water used as heat transfer fluid. Suspending the CuO nanoparticles in water (base fluid) to prepare MNFs appreciably augment the thermal conductivity. The increment attained in the base fluid thermal conductivity due to nanoparticle addition/suspension depends significantly on the concentration of the latter in the former i.e., higher the nanoparticle concentration (in the base fluid), higher

will be the increment attained in the thermal conductivity. The glass temperature in the Cases 3-5 were found to be almost similar to that of Cases 1, 2 respectively. The maximum increment attained in the distillate water yield was found to be about 53.30%, 78.80% and 62.05% using

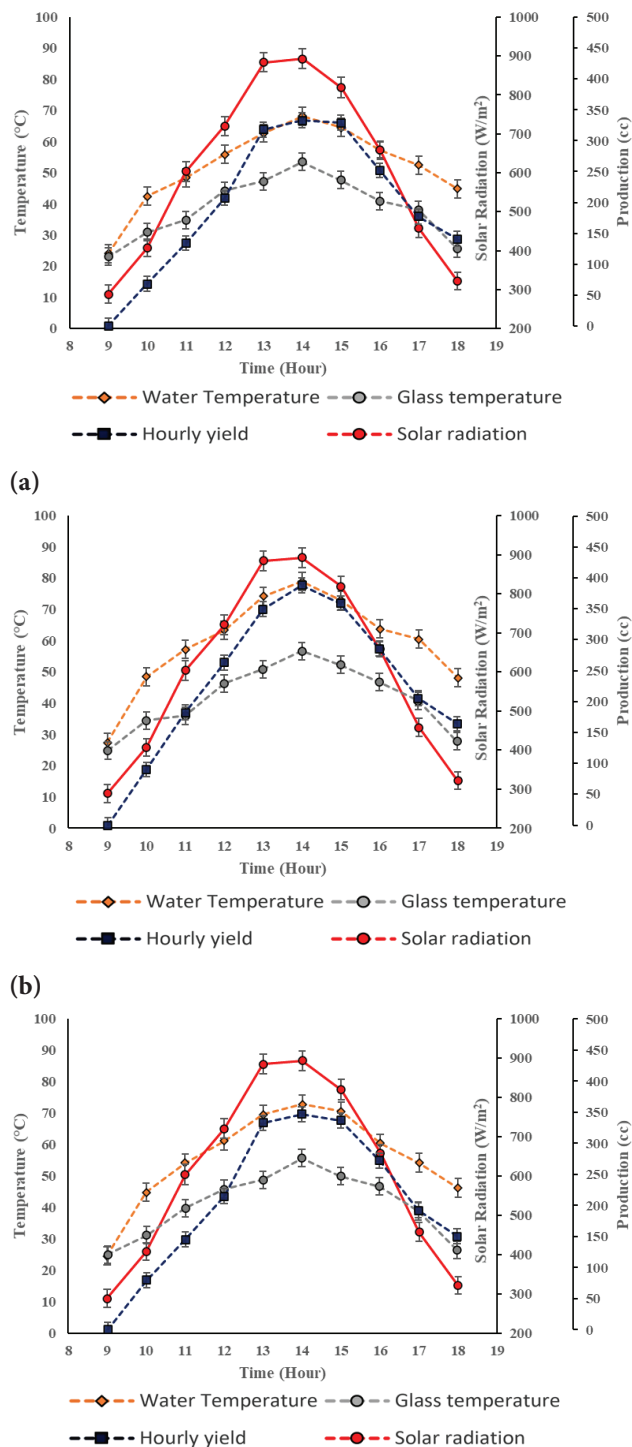


Figure 7. Variation of hourly yield and temperatures of solar still with solar intensity using (a) MNF-1 (Case 3), (b) MNF-2 (Case 4), (c) MNF-3 (Case 5) in the heater.

MNF-1 (Case 3), MNF-2 (Case 4) and MNF-3 (Case 5) respectively as the heat transfer fluids. It is clear that out MNF 1-3, the maximum increment in the distillate water yield was attained using MNF-2. This can be attributed to the trade-off attained between the dynamic viscosity and thermal conductivity at 1.0 wt.% concentration in CuO MNF. Hence, the 1.0 wt.% concentration was taken as the optimum nanofluid concentration and all the HNFs used in this study were prepared to be of 1.0 wt.% concentration.

Figures 8 (a)-(c) illustrate the hourly variation in the water, glass temperatures and distilled water yield of solar heater coupled still with solar irradiation intensity employing HNF-1 (Case 6), HNF-2 (Case 7) and HNF-3 (Case 8) respectively as the heat transfer fluids. Employing hybrid nanofluids within the heater significantly augments the performance of the coupled solar still. Experimenting with the hybrid nanofluids, higher saline water temperatures were realized relative to that attained in Cases (1-5). This can be attributed to the superior thermal and flow properties of HNFs relative to that of the MNF (1-3) and base fluid (water). The increment in the water temperature resulted in augmenting the distillate water yield due to realization of higher evaporation rates. The water temperature and the distillate water yield were found to showcase sharp slopes during the initial hours of the experiment attributed to the increasing solar irradiation intensity and the support of using hybrid nanofluids in the heater. It was found that the solar still performance improved with the increase in the proportion of GO nanoparticles in the HNFs. Since, a maximum increment attained in the distillate water yield were found to be about 89.30%, 101.33% and 127.46% in the Cases 6,7 and 8 respectively relative to that attained in the Case 1 (conventional solar still) regarded to the high thermal conductivity of the GO nanoparticles. This resulted in higher thermal conductivity of the HNFs having larger proportion of GO nanoparticles. Realization of the increasing thermal conductivity of HNFs with the increase in the GO nanoparticle concentration resulted in efficient transfer of the heat energy absorbed by the hybrid nanofluids (in the solar heater) to the saline water. Improved supply of heat energy to the saline water increased its temperature which improved its evaporation rate further resulting in the improved hourly productivity or the distillate water yield of the solar still. The glass temperatures were observed to remain almost similar in the Cases 6-8. However, slight increment in the same was observed relative to that attained in the Case 1 attributed to augmented realization of water vapour condensation rates within the solar still on the inner glass surface and the increment in the solar irradiation intensity during the final days of the experiment due to progression of summer season with the passing days.

It was observed during the experiments that the concentration, proportions of the nanoparticles added in the base fluid influence the performance of the solar still if utilized as the heat transfer fluids. This can be stated by the fact that out of all the prepared CuO MNFs, the 1.0 wt.%

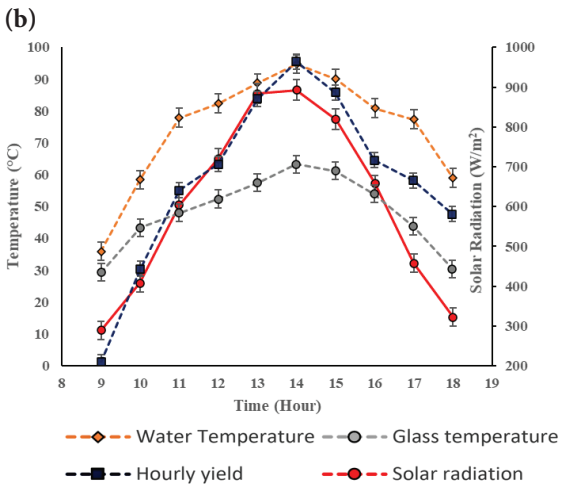
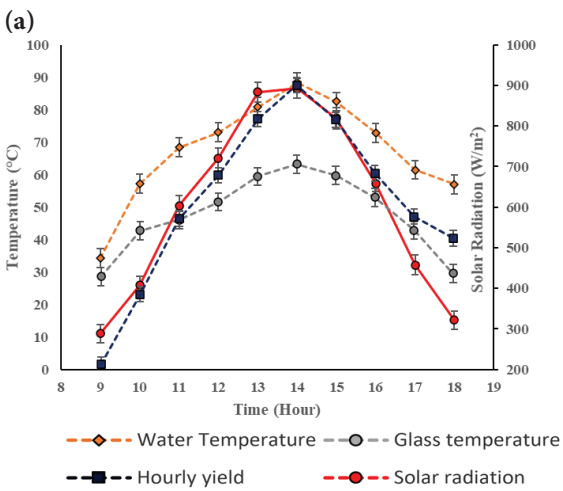
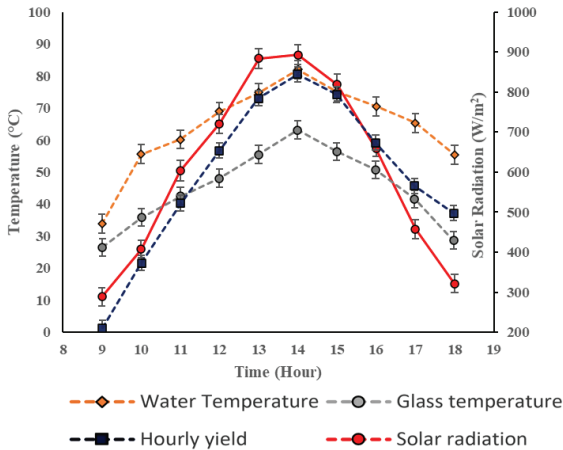


Figure 8. Variation of hourly yield and temperatures of solar still with solar intensity using (a) HNF-1 (Case 6), (b) HNF-2 (Case 7), (c) HNF-3 (Case 8) in the heater.

concentration was found to be optimum to attain best solar still performance out of the Cases 1-5. Another supporting fact for the same is that the best solar still performance was realized using HNF-3 as the heat transfer fluid i.e., Case 8 out of the Cases 1-8 respectively. This was attributed to the

higher thermal conductivity of the HNFs with higher concentration of GO nanoparticles. But it was realized during the experiments that if the key to attain superior solar still performance is the utilization of higher proportions of high thermal conductivity GO nanoparticles, then the 1.0 wt.% GO (MNF-4) could result in further augmentation in the productivity of the solar still. Therefore, later in the study, 1.0 wt.% GO nanofluids were also tested for their employability as the heat transfer fluid in the solar heater coupled still.

Figure 9 illustrates the hourly variation in the water, glass temperatures and distilled water yield of solar heater coupled still with solar irradiation intensity using MNF-4 (Case 9). It was observed during the experiment that employing the MNF-4 as the heat transfer fluid in the experimental set-up improved the performance of the solar still relative to that attained in the Case 1 with the attainment of a maximum increment of about 54.93% in the distillate water yield. However, upon further comparison with the Cases 2-8, it was observed that the performance augmentation attained in the Case 9 could only surpass that attained in the Cases 2, 3 respectively i.e., using water and MNF-1 as the heat transfer fluids with an increment of about 20.30%, 1.07% respectively in the distillate water yield. It was clear post that HNFs pose higher potential for performance augmentation of the solar still relative to the MNFs and water.

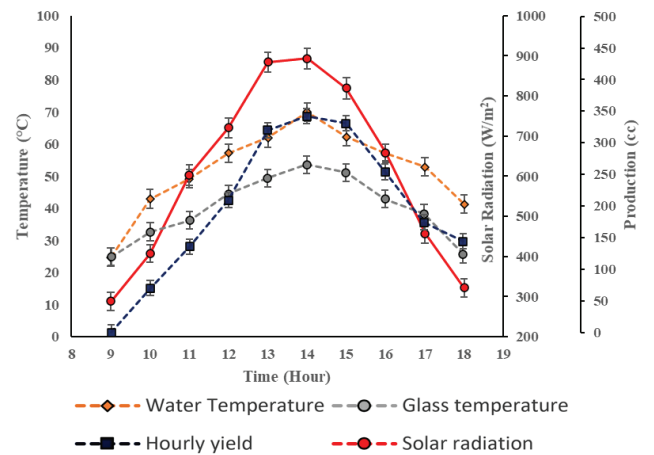


Figure 9. Variation of hourly yield and temperatures of solar still with solar intensity using MNF-4 in the heater.

It gets clear from the discussion that solar heater coupled still offer better productivity relative to that attained in the conventional solar still attributed to superior thermal and flow properties of heat transfer fluids and enriched availability of thermal energy for the saline water. The pumping power required to circulate the different heat transfer fluids through a close loop between the solar still and solar heater is an essential parameter to be considered during the selection of the best performing heat transfer fluid. An ideal heat

transfer fluid for such application would be the one resulting high distillate water yield of solar still with minimum pumping power required to maintain its circulation. It is crucial to minimize the required pumping power of heat transfer fluids to make the solar heater coupled still set-up operable from the economic perspectives.

During the experiments it was observed that the pumping power of the nanofluids (used as the heat transfer fluids in the current study) varied with the variation in the nanofluid physical properties. Since, the pumping power required in Case 2 was quite lower relative to that in Cases 3-9 attributed to the lower dynamic viscosity of water. Suspension of nanoparticles in the base fluid increases its dynamic viscosity. The high dynamic viscosity of nanosuspensions results in higher flow resistance. This eventually poses requirement of high pumping power to maintain the fluid flow. Such increment in the pumping power due to increased dynamic viscosity can be regarded as the function of the nanoparticle type, its shape, size and its concentration in the base fluid. The flow characteristics of the base fluid also influence the same of their nanofluids. It was observed post experimentation that the pumping power required for different heat transfer fluids and the advantage attained using them in terms of augmented distilled water yield contradict each other during the selection of best performing heat transfer fluid. Hence, the authors decided to assess the performance index for different heat transfer fluids.

The performance index of a heat transfer fluid contrasted in this study was defined as the “distillate water yield of solar heater coupled still (in cc) per unit pumping power consumption of the heat transfer fluid (in Watts)”. Figure 10 illustrates the comparison of the performance index and distillate water yield of different heat transfer fluids tested in the current study. Out of all the tested heat transfer fluids, the maximum fresh water yield was attained using HNF-3 (2907 cc) followed by HNF-2 (2573 cc), HNF-1 (2419 cc), MNF-2 (2285 cc), MNF-3 (2071 cc), MNF-1 (1959 cc), water (1646 cc). However, it gets clear after assessing the performance indices of all the heat transfer fluids that HNF-2 was the most suitable out of all the tested heat transfer fluids in the experimental set-up. Since the maximum performance index of 134.64 cc/W was attained using HNF-2 followed by HNF-3 (127.22 cc/W), HNF-1 (126.71 cc/W), MNF-2 (120.26 cc/W), MNF-1 (104.75 cc/W), MNF-3 (98.61 cc/W) and water (91.44 cc/W) respectively in the set-up. HNF-3 offered the maximum distillate water yield but considering the pumping power, HNF-2 can be regarded as the most suitable heat transfer fluid since it realized the maximum performance index i.e., maximum distillate water yield for unit pumping power consumption out of all the tested heat transfer fluids.

The nanofluids offer high thermophysical properties when utilized as heat transfer fluids. It is the reason that when the nanofluids are filled in the tubes of the solar heater, then they readily gain the thermal energy of the

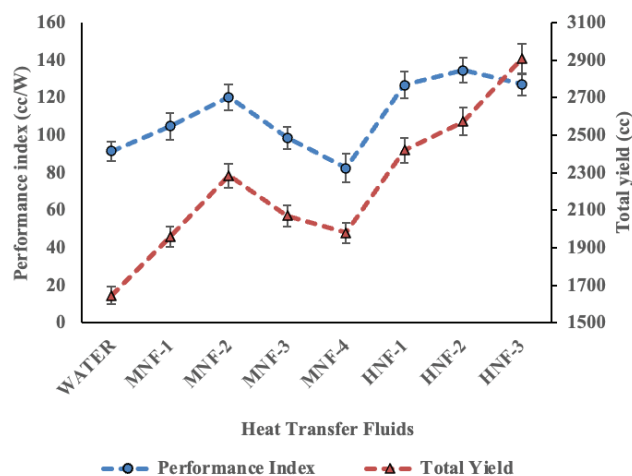


Figure 10. Variation of productivity index and total yield attained using different heat transfer fluids.

incident solar radiation and store it in the form of sensible heat. The high temperature nanofluid when pumped through the tubes from the solar heater to the saline water then the former rejects its sensible heat to the surrounding saline water. This increases the saline water temperature further augmenting its vaporization rate while the cooled nanofluid is pumped back to the solar heater to carry out its cyclic flow. The nanofluid after coming in indirect contact with the saline water, reject significant amount of the absorbed thermal energy by virtue of its advance thermo-physical properties (high thermal conductivity, heat transfer coefficient) and the nanoparticle Brownian motion. The Brownian motion i.e., the random motion of nanoparticles across the base fluid result in improved heat transfer towards the enclosing channel or tube, further transferred to the surrounding saline water.

The density of the nanofluid employed in the heater also influences the performance of the coupled solar still. There exists an optimum nanofluid concentration which optimizes the distillate water yield of the solar still. Such concentration of nanofluid acts to be optimum when a favorable trade-off is attained between its thermal properties and viscosity. With the increase in the nanofluid concentration, the thermal characteristics of the nanofluid improves correspondingly. However, the same also results in increased dynamic viscosity of the nanofluid. The increment in the viscosity reduces its mass flow rate through the tube (measured in the form of pressure drop across the orifice plate). The reduction in the mass flow rate results in reduced heat rejection from the nanofluid to the saline water which degrades its evaporation rate and finally the distillate water yield in the solar still.

Hence a trade-off should be attained between the improved thermal characteristics and degraded flow characteristics of the nanofluid such that maximum heat transfer occurs from the nanofluid to the saline water and

Table 3. Total fixed cost for different experimental cases

Case	Experimental set-up	Heat transfer fluid	Total fixed cost (\$)
Case 1	Conventional solar still	Not applicable	98
Case 2	Solar heater coupled solar still	DI water	133
Case 3	Solar heater coupled solar still	MNF-1	175
Case 4	Solar heater coupled solar still	MNF-2	183
Case 5	Solar heater coupled solar still	MNF-3	194
Case 6	Solar heater coupled solar still	HNF-1	202
Case 7	Solar heater coupled solar still	HNF-2	224
Case 8	Solar heater coupled solar still	HNF-3	253
Case 9	Solar heater coupled solar still	MNF-4	289

improves the distillate water yield in the solar still by realizing high evaporation rates. Such optimization between the thermal and flow characteristics in the current study was attained using HNF-2 at 1.0 wt.% concentration and 50:50 proportion of CuO and GO nanoparticles in water.

Economic Analysis

Herein the authors have tried to compare all the Cases (1-9) from economy point of view. The total fixed costs (F) of the experimental set-up in the considered cases are tabulated in Table 3.

Assuming the system lifetime (n) to be 10 years and interest rate (i) of 15%, the equations involved in the economic analysis were [26]:

The capital recovery factor (CRF), fixed annual cost (FAC) is evaluated as,

$$CRF = \frac{i(1+i)^n}{(1+i)^n - 1} \quad (3)$$

$$FAC = F * (CRF) \quad (4)$$

The Sinking fund factor (SFF) is evaluated as,

$$SFF = \frac{i}{(1+i)^n - 1} \quad (5)$$

The salvage value (S) and annual salvage value (ASV) is evaluated as,

$$S = 0.2 * F \quad (6)$$

$$ASV = S * (SFF) \quad (7)$$

The annual maintenance cost (AMC) is evaluated as,

$$AMC = 0.15 * (FAC) \quad (8)$$

The total annual cost (TAC) is evaluated as,

$$TAC = FAC + AMC - ASV \quad (9)$$

Finally, the distilled water cost per litre (CPL) is evaluated as,

$$CPL = \frac{TAC}{\text{Average yearly fresh water yield}} \quad (10)$$

Following the equations (3-8), the CPL for Cases (1-9) were found to be about 0.028, 0.026, 0.022, 0.018, 0.023, 0.016, 0.013, 0.015, 0.022 \$/L respectively.

Water Quality Assessment

The quality of the saline water and that of the distillate water produced from the experimental set-up when operated using HNF-2 (i.e., Case 7) was compared with the Bureau of Indian Standards (BIS). The measurement of the total dissolved solids (TDS) content, conductivity, pH and fluoride composition of the saline water sample and distillate water sample (of Case 7) was carried out. The results for the specified measurements are tabulated in the Table 4. It is clear from the results presented in the Table 4 that the produced distilled water was suitable for the human consumption. However, with the addition of essential minerals in the produced distilled water, it will completely fulfill the criteria as directed by the BIS.

Table 4. Water quality comparison with BIS data

Quality parameter	Saline water	Distilled water (of Case 7)	BIS Standard [27]
TDS (ppm)	921	12	250-320
Conductivity (μ S/cm)	884	31	0-800
pH	6.1	7.2	6.5-8.5
Fluoride content (ppm)	1.9	0.2	0.1-1.0

CONCLUSION

A square basin pyramid solar still was coupled with a solar heater to augment its performance. Different heat transfer fluids were tested and compared in the set-up to maximize the distillate water yield followed by the evaluation of performance index and economy analysis for their respective cases. Following are the key conclusions drawn from the study:

- The distillate water yield of conventional solar still tend to be quite limiting and were found to be least out of all the tested cases attributed to lower availability of the heat transfer area.
- Coupling the solar still with a solar heater augments the distillate water yield. Utilizing DI water in the solar heater results in the improvement of about 28.80% in the distillate water yield.
- The distillate water yield of the coupled system was found to be the function of the concentration of employed mono-nanofluid in the solar heater.
- The maximum increment of about 78.80% was attained in distillate water yield relative to the conventional solar still by utilizing the 1.0 wt.% CuO mono-nanofluid while that offered by the 0.5 wt.% and 1.5 wt.% CuO mono-nanofluid was found to be about 53.30% and 62.05% respectively.
- The distillate water yield of the coupled system was found to be the function of the nanoparticle proportion for a given hybrid nanofluid concentration in the solar heater.
- The utilization of (25:75) CuO+GO hybrid nanofluid in the solar heater resulted in the maximum increment of about 127.46% in the distillate water yield of the solar still followed by (50:50) CuO+GO hybrid nanofluid (i.e., 101.33%) and (75:25) CuO+GO hybrid nanofluid (i.e., 89.30%) respectively.
- Employing the 1.0 wt.% GO mono-nanofluid in the heater resulted in an increment of just 54.93% in the distillate water yield relative to that of the conventional solar still.
- The pumping power requirement of the prepared nanosuspensions varied with the nanoparticle composition.
- All the utilized heat transfer fluids were compared in terms of their respective performance indices calculated as distillate water yield per unit pumping power.
- The performance index of the (50:50) CuO+GO hybrid nanofluid was observed to be the most proficient out of all the tested heat transfer fluids since it offered the maximum distillate water yield for unit pumping power input. This can be attributed to the optimized trade-off attained between its thermal, flow characteristics at the given nanoparticle concentration and proportion.

- The results of the economy analysis of the experimental set-up for different cases suggested that the least cost per unit distillate water yield was found to be about 0.013 \$/L in Case 7 when the heater was filled with the (50:50) CuO+GO hybrid nanofluid.
- The potential heat transfer fluid for realizing best system performance of the solar still is the (50:50) CuO+GO hybrid nanofluid both from the productivity and economy perspectives.

Scope for Future Work

Significant research work has been reported by the scientific community to enhance the distillate water yield of the solar water desalination systems. Following are some of the recommendations for the future research objectives to promote further advancement in the performance of the solar stills.

- Investigation for more efficient nanoparticle combinations should be carried out to further enhance the performance of solar stills.
- The prevailing phenomena behind the noteworthy performance characteristics of the hybrid nanofluids is needed to be further investigated for better understanding the involved heat transfer mechanisms.
- The exergy and energy analysis of hybrid nanofluids requires exploration.
- More efficient structural designs of the solar desalination systems are required to be devised.
- Proper material selection can be carried out to promote drop wise condensation in the still to achieve better heat transfer.

AUTHORSHIP CONTRIBUTIONS

Authors equally contributed to this work.

DATA AVAILABILITY STATEMENT

The authors confirm that the data that supports the findings of this study are available within the article. Raw data that support the finding of this study are available from the corresponding author, upon reasonable request.

CONFLICT OF INTEREST

The author declared no potential conflicts of interest with respect to the research, authorship, and/or publication of this article.

ETHICS

There are no ethical issues with the publication of this manuscript.

REFERENCES

- [1] Damkjaer S, Taylor R. The measurement of water scarcity: Defining a meaningful indicator. *Ambio* 2017;46:513–531. [\[CrossRef\]](#)

- [2] Chen X, Shuai C, Wu Y, Zhang Y. Understanding the sustainable consumption of energy resources in global industrial sector: Evidences from 114 countries. *EIA Review* 2021;90:106609. [CrossRef]
- [3] Abdelgaied M, Kabeel AE, Kandeal AW, Abosheisha HF, Shalaby SM, Hamed MH, et al. Performance assessment of solar PV-driven hybrid HDH-RO desalination system integrated with energy recovery units and solar collectors: Theoretical approach. *Energy Convers Manag* 2021;239:114215. [CrossRef]
- [4] Shoeibi S, Rahbar N, Esfahlani AA, Kargarsharifabad H. A comprehensive review of Enviro-Exergo-economic analysis of solar stills. *Renew Sustain Energy Rev* 2021;149:111404. [CrossRef]
- [5] Alawee WH, Essa FA, Mohammed SA, Dhahad HA, Abdullah AS, Omara ZM, et al. Improving the performance of pyramid solar distiller using dangled cords of various wick materials: Novel working mechanism of wick. *Case Stud Therm Eng* 2021;28:101550. [CrossRef]
- [6] Essa FA, Alawee WH, Mohammed SA, Abdullah AS, Omara ZM. Enhancement of pyramid solar distiller performance using reflectors, cooling cycle, and dangled cords of wicks. *Desalination* 2021;506:115019. [CrossRef]
- [7] Hansen RS, Munaf AA, Allasi HL, Endro S, Leno J, Kanna SKR. Experimental and theoretical optimization of an inclined type solar still using PV sustainable recirculation technique. *Mater Today Proc* 2021;45:7063–7071. [CrossRef]
- [8] de Paula ACO, Ismail KAR. Comprehensive investigation of water film thickness effects on the heat and mass transfer of an inclined solar still. *Desalination* 2021;500:114895. [CrossRef]
- [9] Elmaadawy K, Kandeal AW, Khalil A, Elkadeem MR, Liu B, Sharshir SW. Performance improvement of double slope solar still via combinations of low cost materials integrated with glass cooling. *Desalination* 2021;500:114856. [CrossRef]
- [10] Parsa SM, Yazdani A, Dhahad H, Alawee WH, Hesabi S, Norozpour F, et al. Effect of Ag, Au, TiO₂ metallic/metal oxide nanoparticles in double-slope solar stills via thermodynamic and environmental analysis. *J Clean Prod* 2021;311:127689. [CrossRef]
- [11] Toosi SSA, Goshayeshi HR, Heris SZ. Experimental investigation of stepped solar still with phase change material and external condenser. *J Energy Storage* 2021;40:102681. [CrossRef]
- [12] Elsheikh AH, Katekar VP, Muskens OL, Deshmukh SS, Elaziz MA, Dabour SM. Utilization of LSTM neural network for water production forecasting of a stepped solar still with a corrugated absorber plate. *Process Saf Environ Prot* 2021;148:273–282. [CrossRef]
- [13] Shoeibi S, Rahbar N, Esfahlani AA, Kargarsharifabad H. A review of techniques for simultaneous enhancement of evaporation and condensation rates in solar stills. *Sol Energy* 2021;225:666–693. [CrossRef]
- [14] Attia MEH, Kabeel AE, Abdelgaied M, Shmouty AR. Enhancing the hemispherical solar distiller performance using internal reflectors and El Oued sand grains as energy storage mediums. *Environ Sci Pollut Res* 2021;29:21451–21464. [CrossRef]
- [15] Khalilmoghadam P, Rajabi-Ghahnavieh A, Shafii MB. A novel energy storage system for latent heat recovery in solar still using phase change material and pulsating heat pipe. *Renew Energy* 2021;163:2115–2127. [CrossRef]
- [16] Younes MM, Abdullah AS, Essa FA, Omara ZM, Amro MI. Enhancing the wick solar still performance using half barrel and corrugated absorbers. *Process Saf Environ Prot* 2021;150:440–452. [CrossRef]
- [17] Tuly SS, Rahman MS, Sarker MRI, Beg RA. Combined influence of fin, phase change material, wick, and external condenser on the thermal performance of a double slope solar still. *J Clean Prod* 2021;287:125458. [CrossRef]
- [18] Amiri H, Aminy M, Lotfi M, Jafarbeglo B. Energy and exergy analysis of a new solar still composed of parabolic trough collector with built-in solar still. *Renew Energy* 2021;163:465–479. [CrossRef]
- [19] Nazari S, Safarzadeh H, Bahiraei M. Performance improvement of a single slope solar still by employing thermoelectric cooling channel and copper oxide nanofluid: An experimental study. *J Clean Prod* 2019;208:1041–1052. [CrossRef]
- [20] Shoeibi S, Rahbar N, Esfahlani AA, Kargarsharifabad H. Improving the thermoelectric solar still performance by using nanofluids- Experimental study, thermodynamic modeling and energy matrices analysis. *Sustain Energy Technol Assess* 2021;47:101339. [CrossRef]
- [21] Abdelgaied M, Zakaria Y, Kabeel AE, Essa FA. Improving the tubular solar still performance using square and circular hollow fins with phase change materials. *J Energy Storage* 2021;38:102564. [CrossRef]
- [22] Abdelaziz GB, Algazzar AM, El-Said EMS, Elsaid AM, Sharshir SW, Kabeel AE, et al. Performance enhancement of tubular solar still using nano-enhanced energy storage material integrated with v-corrugated aluminum basin, wick, and nanofluid. *J Energy Storage* 2021;41:102933. [CrossRef]
- [23] Abdelgaied M, Attia MEH, Kabeel AE, Zayed ME. Improving the thermo-economic performance of hemispherical solar distiller using copper oxide nanofluids and phase change materials: Experimental and theoretical investigation. *Sol Energy Mater Sol Cells* 2022;238:111596. [CrossRef]
- [24] Shoeibi S, Kargarsharifabad H, Rahbar N, Ahmadi G, Safaei MR. Performance evaluation of a solar still using hybrid nanofluid glass cooling-CFD simulation and environmental analysis. *Sustain Energy Technol Assess* 2022;49:101728. [CrossRef]

-
- [25] Rabbi HMF, Sahin AZ. Performance improvement of solar still by using hybrid nanofluids. *J Therm Anal Calorim* 2021;143:1345-1360. [\[CrossRef\]](#)
- [26] Essa FA, Alawee WH, Mohammed SA, Dhahad HA, Abdullah AS, Omara ZM. Experimental investigation of convex tubular solar still performance using wick and nanocomposites. *Case Stud Therm Eng* 2021;27:101368. [\[CrossRef\]](#)
- [27] Thakur AK, Sathyamurthy R, Velraj R, Saidur R, Hwang JY. Augmented performance of solar desalination unit by utilization of nano-silicon coated glass cover for promoting drop-wise condensation. *Desalination* 2021;515:115191. [\[CrossRef\]](#)